

Supplementary methods.

Photogrammetry methods

We used a combination of digital images and laser measurements to estimate branch diameter. We first took photographs of each branch such that the axis of each diameter measurement was parallel to the x or y axis of the photograph (Powershot ELPH 130IS, Canon, USA). We then used a commercially available laser rangefinder (Disto D5, Leica Geosystems, Austria) to measure distance between the camera and the midpoint of the diameter measurement. Using ImageJ software and known camera characteristics, we then calculated a first estimate of branch diameter, D (in m), as

$$D = \frac{z * l_s}{l_f} * \frac{P_b}{P_a}$$

where z is the distance (m) between the camera and the branch, l_s is the length of the image sensor (mm), l_f is the focal length when taking the photo (mm), P_b is the width of the branch (in pixels), and P_a is the width of the image along the same axis as the branch diameter measurement (in pixels).

To test the accuracy and precision of our photogrammetry measurements, we performed a pilot study of 48 branches that were within reach of the forest floor and measurable by hand. We measured these branches over distances that were representative of our measurements while estimating suspended WD (up to 35m). This method of diameter estimation was both accurate (average difference from real diameter = 0.44 cm) and precise (SD of difference between real and estimated diameters = 0.2 cm) for stems >5cm in diameter ($F_{1,46} = 3368$, $p < 0.001$, $r^2 = 0.99$). The relationship between estimated and real diameter was consistent regardless of distance between the camera and branch (up to 35m; $F_{1,46} = 2.40$, $p = 0.13$) and across a range of branch diameters (5-65cm; $F_{1,46} = 1.03$, $p = 0.32$).

We used the Law of Cosines to estimate branch length. We measured distance to both ends of the branch or branch subsection, and estimated the angle between the two measurements using a protractor and plumb line. We then calculated branch length as follows,

$$L_b = d_a^2 + d_b^2 - 2d_a d_b \cos C$$

Where L_b is the length of the branch, d is the distance to each end of the branch (subscripts a and b denote each measurement), and C is the angle between the distance measurements.

Wood density

We performed destructive sampling of woody debris in 2010 to quantify wood density and describe the relationship between real density and penetration with the dynamic penetrometer. By wood density, we mean the oven-dry dry mass divided by the fresh volume. To estimate density of wood cross-sections, we used a disk removal approach that accounted for void space and heterogeneity in wood structure and decomposition. Specifically, we removed a ca. 3cm thick cross-sectional disk from the sample woody debris and returned this disk to the lab. Disk volume was estimated as the diameter multiplied by the average of 5 disk thickness measurements, with the mean edge thickness measurement weighted twice as much as center point thickness. If disks were too large to be returned to the lab, then the entire disk was weighed in the field and a subsection of this disk (200-1000g) was removed. Each section or

subsection was weighed while fresh, dried at 60 °C, and then reweighed to estimate dry density. For subsampled disks, we assumed that the proportion of dry density in the subsample was representative of the entire disk and prorated field-measured fresh mass accordingly. We calculated cross-sectional mass as the cross-sectional area multiplied by the density, as estimated using a variety of different approaches (Larjavaara and Muller-Landau 2011).

We used linear regression to establish the relationship between penetrometer penetration per hit (mm) and dry density (kg m⁻³). For penetrometer penetration relative to dry density, both variables were log transformed to improve normality and linearity. Because the regression was performed with log-transformed wood density as the response variable, we multiplied by a correction factor [$\exp(\text{"squared residual error"}/2)$] when converting from penetration to density in all cases when only penetration was known (Chave and others 2005).

Calculations of mass and volume

We summed squared diameter and cross-sectional area to estimate volume and mass of downed woody debris, respectively. We estimated total volume of downed coarse and fine woody debris from transect data assuming circular cross sections,

$$V = \frac{\pi}{4 \cdot L} \sum D_i^2$$

Where V is volume of woody debris per area (m³ per m⁻²), L is the total length of transects (m), and D_i is diameter (m) of the ith piece of wood encountered (De Vries 1986). We estimated the mass of downed woody debris with individual density estimates and used cross-section mass to account for void space and wood heterogeneity,

$$M = \frac{1}{L} \sum C_i$$

Where M is mass of woody debris per area (kg m⁻²), L is the total length of transect (m), and C_i is the cross section mass (kg m⁻¹) for the ith piece of wood. Cross-section mass equals mass divided by the length of the sample, or equivalently the product of cross-section area and dry density (kg m⁻³) as estimated via disk sampling or penetrometer penetration (Larjavaara and Muller-Landau 2011). Equations 2 and 3 include were corrected to account for the angle of each WD piece, but these corrections differed by sampling type. For unidirectional transects (i.e., 2010 and 2014 long transects), we divided cross-sectional mass (or cross-sectional area) by sine of the angle between the longitudinal axis of the piece of WD and the transect itself to account for the orientation of diameter measurements relative to the piece of CWD rather than the transect itself. For all other downed woody debris datasets, we multiplied sample cross-sectional mass and cross-sectional area by the random angle correction factor ($\pi/2$).

Exponential decay

We estimated decomposition constants of individual pieces of CWD. The decomposition rate, k_i, of the ith sample was calculated from the initial and final cross-section mass, c_{i,0} and c_{i,t} and the elapsed time t assuming an exponential decay model:

$$c_{i,0} = c_{i,t} \exp(-k_i t)$$

thus,

$$k_i = \ln\left(\frac{c_{i,0}}{c_{i,t}}\right) * \frac{1}{t}$$

Cross-section mass was replaced by volume, mass, or cross-section area when applicable. To estimate residence time from these individualized measurements, decay constants were averaged for individual pieces of CWD that were remeasured and then weighted by the original mass and cross-sectional mass of each piece of standing and downed CWD, respectively.

Derivation of corrected inputs

Variable definitions:

$N(t)$ = the quantity of material in a woody debris pool of interest at time t (units are mass per area, volume per area, cross-sectional mass per area, or cross-sectional area per area). This is what is recorded in the field.

$S(t)$ = the “surviving” quantity of woody debris at time t that was already present at time 0 (after losses to decomposition and to falling below the size threshold for inclusion)

$I(t)$ = the quantity of material measured at time t that was new to the pool since time zero (that is, the flux in that has not yet decomposed below the size threshold).

**Note that $N(t)$, $S(t)$, and $I(t)$ all have the same units.

$r(t)$ = the instantaneous rate of loss from the pool at time t , including both decomposition and falling beneath the size threshold for inclusion (in units of quantity per time). Note that by this definition, the true instantaneous flux out of the pool is $N_{out}(t) = r(t)N(t)$, with units of quantity per time.

$g(t)$ = the instantaneous input rate of woody debris into the pool of pieces above the minimum size threshold at time t (in units of quantity per time). Note that by definition, this is the true flux into the pool: $N_{in}(t) = g(t)$, with units of quantity per time.

We assume a steady-state model (Palace and others 2012) such that rates r and g are constant in time so that $r(t) = \tilde{r}$ and $g(t) = \tilde{g}$, and the system reaches an equilibrium \tilde{N} . In this case, the input flux will equal the output flux:

$$N_{in} = \tilde{g} = \tilde{r}\tilde{N} = N_{out}$$

So that:

$$\tilde{r} = \frac{N_{in}}{\tilde{N}} = \frac{\tilde{g}}{\tilde{N}}$$

and the residence time (T_{res}) is defined as:

$$T_{res} = \frac{1}{\tilde{r}} = \frac{\tilde{N}}{N_{in}}$$

Using these equations we can determine the unbiased estimates of the fluxes into and out of this pool. We know that $I(t)/t$ will be an underestimate of N_{in} , because some of the input will have been lost before it was measured. Paralleling estimates for tree mortality (Kohyama and others 2018), an unbiased estimate of the rate r at which pieces leave the pool is as follows:

$$r = \frac{\log\left(\frac{N(0)}{S(t)}\right)}{t}$$

In the case of our study, $N(0)$ is the total necromass of all woody debris in the pool in the dynamics plots at time 0, $S(t)$ is the total necromass of all of that woody debris surviving above the size threshold to time t (not including newly input pieces), and t is the time elapsed. The fact that pieces are no longer observed when they fall below a size threshold is not a problem; inherently, this is the loss rate that includes this effect, and is simply inversely related to residence time in the pool for pieces larger than that size threshold. This equation can then be manipulated as follows:

$$rt = \log\left(\frac{N(0)}{S(t)}\right)$$

$$\frac{N(0)}{S(t)} = e^{rt}$$

$$\frac{S(t)}{N(0)} = e^{-rt}$$

Therefore, the true input rate (and thus the true flux) can be obtained from the observed input $I(t)$ overtime interval t as:

$$g = \frac{I(t)}{t} \frac{\log\left(\frac{N(0)}{S(t)}\right)}{1 - \left(\frac{S(t)}{N(0)}\right)} = I(t) \frac{r}{1 - e^{-rt}}$$

This formula provides an iterative option for calculating the loss rate r . Recall that:

$$\tilde{r} = \frac{\tilde{g}}{\tilde{N}}$$

We can generate an initial estimate of g as the observed input $I(t)$, calculate r using this equation $\tilde{r} = \frac{\tilde{g}}{\tilde{N}}$, and then re-estimate g using the previous equation $g = I(t) \frac{r}{1 - e^{-rt}}$. This process is then repeated iteratively until the values of r and g converge. Because the loss includes both decomposition and the threshold effect, this provides the residence time in the pool.

Minimum sample size calculation

We used a simple variance-based equation to calculate the minimum sample size needed to estimate a statistic with the desired accuracy and precision:

$$SS = \frac{t^2 CV^2}{D^2}$$

Where t is the student's t statistic at a chosen alpha probability level (0.05 in this study), CV is the observed coefficient of variation among samples, and D is the desired proximity to the tree mean, as a percent of the true mean (10% in this study). That is, the result is the estimated minimum sample size to estimate the true mean value within 10% confidence limits with 95% probability. We performed this calculation using the mean observed CV and as well as using the upper limit and lower limit of the 95% confidence interval calculated for the CV .

Elevated proportion of downed WD: estimates and biases

Estimates of the elevated proportion of downed WD differed substantially between the two methods used in this study. These two datasets differed in both the parts of the landscape that were sampled and in sampling procedures, and both differences could contribute to differences in the estimated proportion elevated.

In terms of location, the 2017 long transects were conducted on the 50 ha plot forest dynamics plot, whereas the 2015 short transects were distributed across all of BCI. The 50 ha plot is located on a plateau that is relatively flat and has an unusually high amount of human traffic as workers monitor the forest dynamics plot. The flat topography means that few topographical features elevate sections of downed WD (Přívětivý and others 2016). Additionally, the normal tendency of a careful field technician is to step on dead logs to avoid encounters with animals (e.g., venomous snakes), which often collapses sections of elevated WD (pers. obs., E.M. Gora). In a relatively well-trafficked area such as a forest dynamics plot, this will cause faster-than-normal rates of collapse for sections of elevated WD. For these reasons, the 2017 long transects are likely to underestimate the proportion of woody debris that is elevated. In contrast, the 2015 short transects were distributed across BCI, covering a topographically more complex landscape that on average is less well-trafficked.

The two datasets also differed in sampling procedures. For the 2017 long transects, each piece was scored based on whether it was elevated at the point where it encounters the transect. Thus, these data enable straightforward estimation of the proportion of all woody debris mass or volume that is elevated. By contrast, for the 2015 short transects, each piece was followed over all connected subunits (diameter was measured at each location that an elevated section reached the soil and the midpoint between each of these locations and/or the end of the piece of WD), and the proportion of its total mass that was elevated was assessed (Fig. S1). We determined the volume of each downed and elevated section using *equation 1* (3 diameter measurements per section). The mean overall proportion elevated was calculated as the weighted mean across pieces encountered, weighting by the mean cross-section area of each piece. This is a nonstandard sampling procedure and the relationship of the resulting estimated mean proportion elevated to the true landscape proportion elevated is unclear. There was no correlation between cross-sectional area (the scaling parameter to correct for the size of encountered pieces of WD) and the proportion of WD volume that is elevated ($t_{175} = 1.57$, $p = 0.12$). However, the proportion of WD that was elevated was weakly positively correlated with WD piece length ($t_{175} = 2.86$, $p = 0.004$, $R = 0.21$), which could contribute to overestimation of

the proportion of downed WD that is elevated considering that longer pieces are more likely to be encountered.

Supplementary results

Mass and density measurements

Based on destructive sampling, average wood density of disks extracted from CWD was 0.271 g cm^{-3} (SD = 0.171 g cm^{-3}) of dry mass per fresh volume, and penetrometer penetration was predictive of this wood density ($F_{1,136} = 68.27$, $p < 0.01$, $r^2 = 0.34$; Fig. S6). Wood density decreased with increasing CWD diameter ($F_{1,133} = 15.94$, $p < 0.001$), but this relationship was weak ($r^2 = 0.1$). Thus, we multiplied volume by average CWD density when piece-specific wood densities were not available. As for CWD pools, standing CWD inputs were substantially denser as estimated from penetrometer measurements (mean \pm SD = $0.350 \pm 104 \text{ g m}^{-3}$) than downed CWD inputs (mean \pm SD = $0.283 \pm 104 \text{ g m}^{-3}$; $t = 9.85$, $df = 699$, $p < 0.001$), suggesting that standing inputs were less decomposed than downed inputs. This likely explained why the volume of downed CWD was substantially larger than standing CWD, but the mass of downed and standing inputs were similar (Fig. 3 and S3).

We compared mass estimates using average density and CWD-specific penetration across 6 years in the 40x40m plots. The mass estimates differed for standing and downed CWD, but the magnitude of this difference was small and the direction was inconsistent. Standing CWD mass was greater when estimated with a penetrometer (dAIC = 9.77, $X^2_1 = 11.77$, $p < 0.001$), whereas downed CWD mass was greater when estimated with average density (dAIC = 7.77, $X^2_1 = 9.77$, $p = 0.002$; Table S2). Because penetrometer-based estimates account for real variation in density, we reported penetrometer-based mass estimates when they are available and average density-based estimates when they were not (Table 1). Disk-extraction estimates of mass were consistent with the other approaches (Table S3).

Supplementary Figures

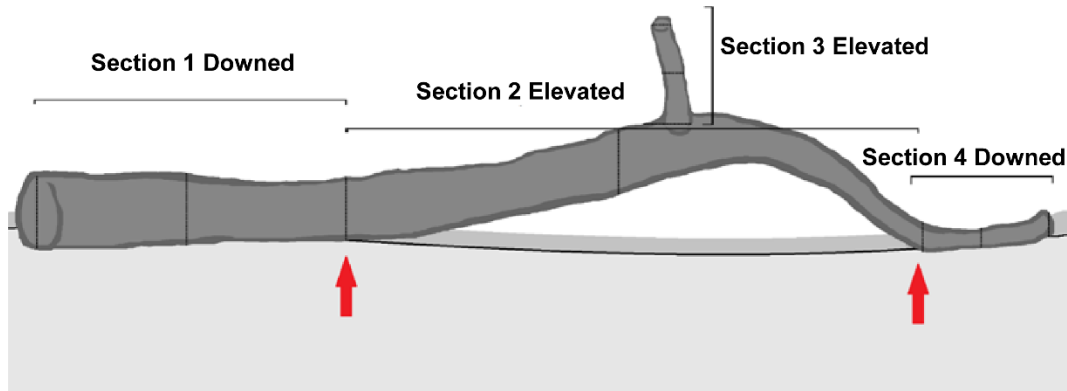


Figure S1. A piece of downed CWD with elevated and downed subsections (each labelled independently). The red arrows indicate the transition point between downed and elevated subsections. The black lines running orthogonally to the longitudinal axis of the branch indicate where measurements were taken to calculate subsection volume using *equation 1*.

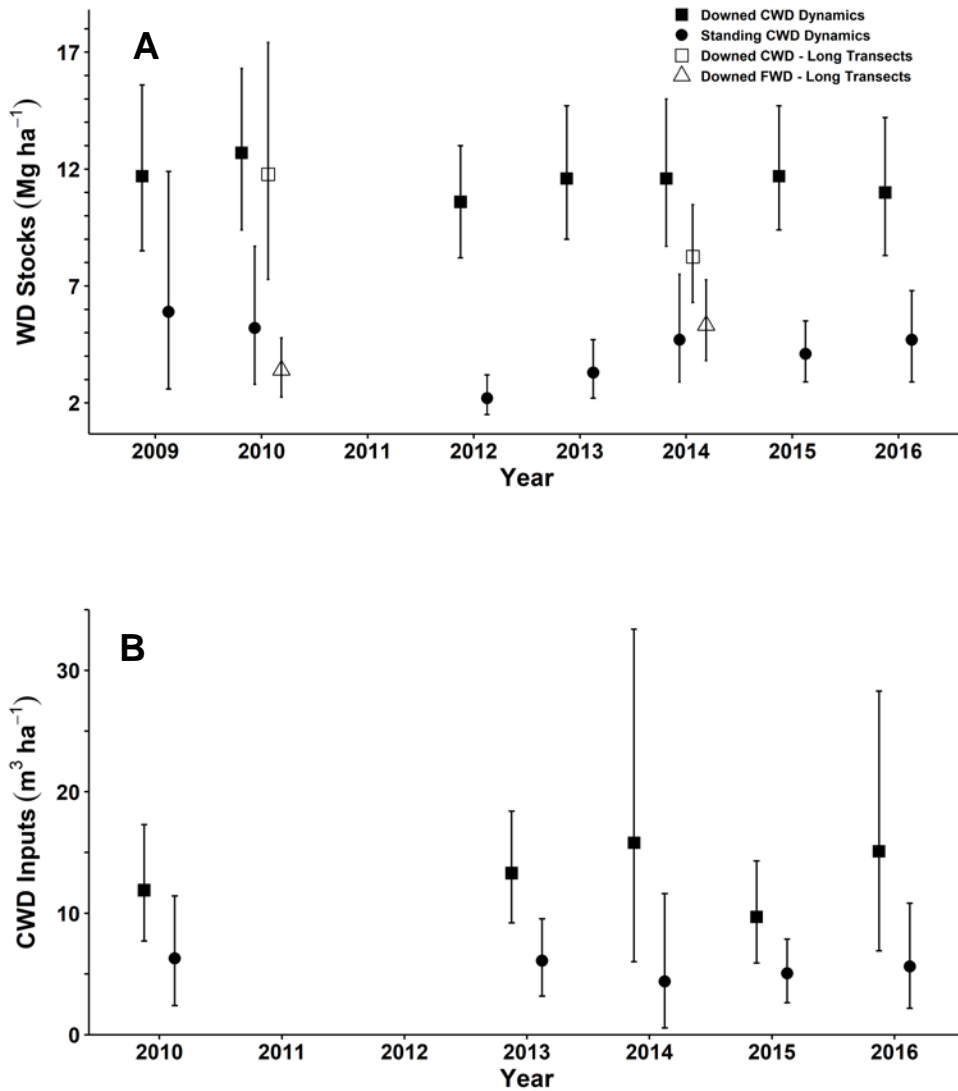


Figure S2. Annual variability in estimated downed and standing CWD stocks (A) and inputs (B) as mass (Mg ha^{-1}) with 95% confidence intervals based on data from the 40x40m dynamics plots (filled symbols). Also presented are estimated stocks from the long transects in 2010, 2014, and 2017 (open symbols). The shaded regions represent the mean volume ($\pm 95\%$ CI) of downed CWD and standing CWD as calculated across all years in the dynamics plots.

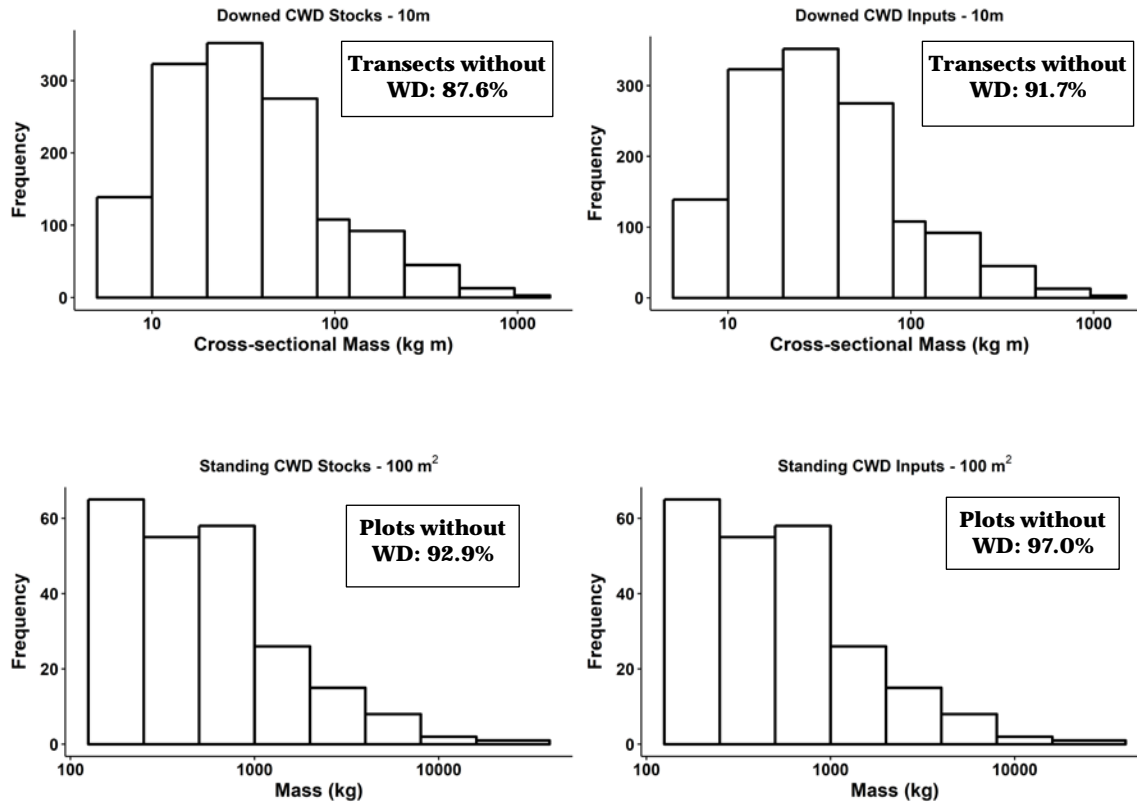


Figure S3. Variation among sampling units in the amount of coarse wood debris (CWD) stocks and inputs across all years combined for the CWD dynamics plots surveys. Cross-sectional mass is the dry mass per cross-sectional area encountered by the sampling transect. Bin size doubles with each increasing increment (0.05 m³, 0.1 m³, 0.2 m³, etc.; 5 kg m, 10 kg m, 20 kg m, etc). The histograms only include transects with WD; the percentage of sampling units without WD is given in text on each panel.

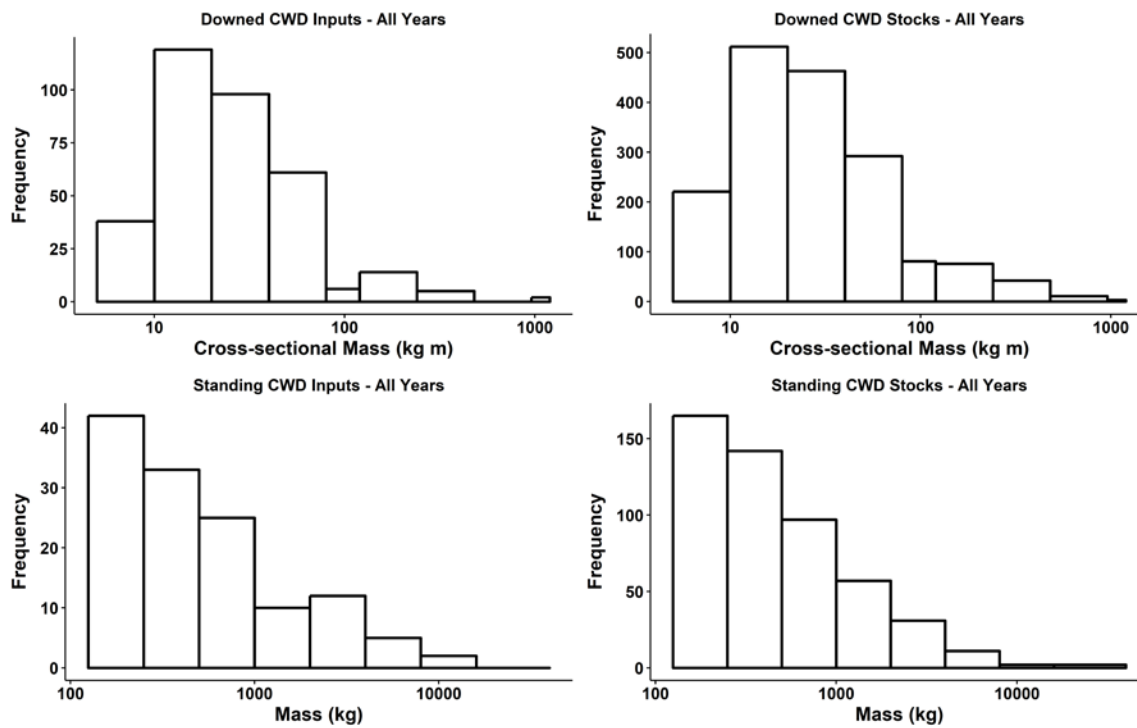


Figure S4. Variation in the cross-sectional mass and mass of individual pieces of downed and standing CWD, respectively. Cross-sectional mass is the dry mass per cross-sectional area encountered by the sampling transect. Pieces of CWD are separated into stocks and inputs, and the x-axis of each plot is log transformed.

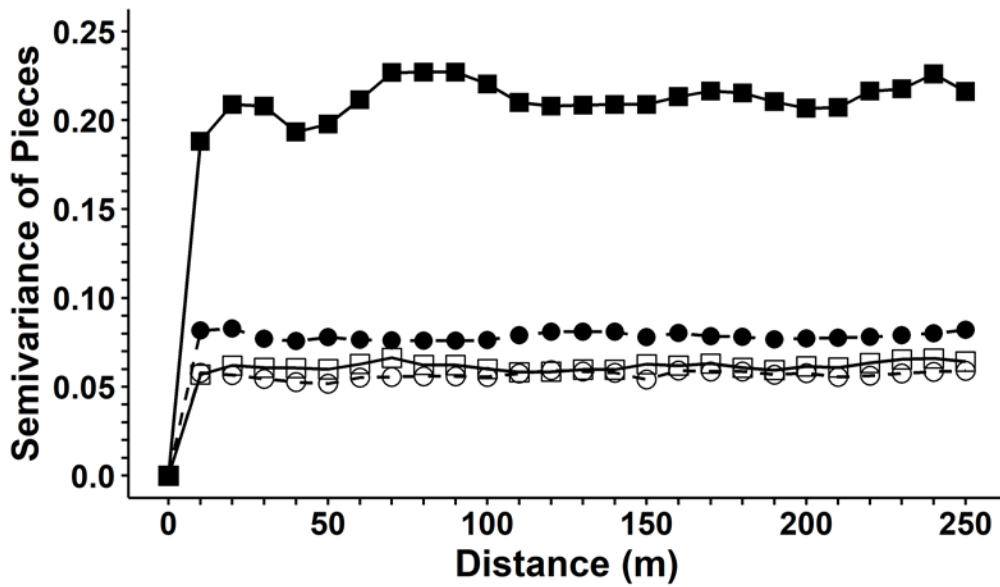
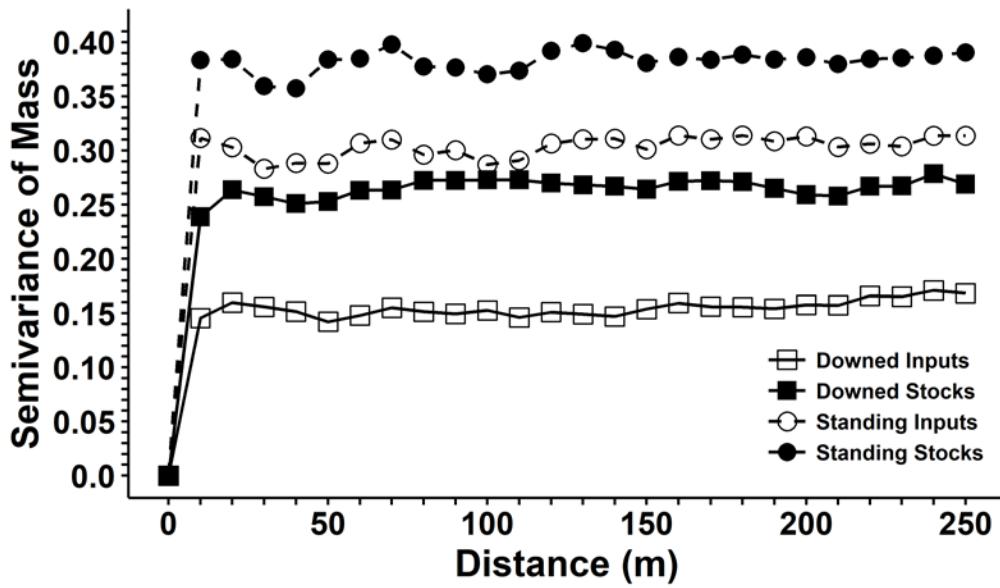


Fig. S5. Semivariogram of stocks (filled points) and inputs (hollow points) of downed and standing CWD mass and CWD pieces. Each point represents the mean over annual semivariograms calculated for 5 or 7 years for inputs and stocks, respectively.

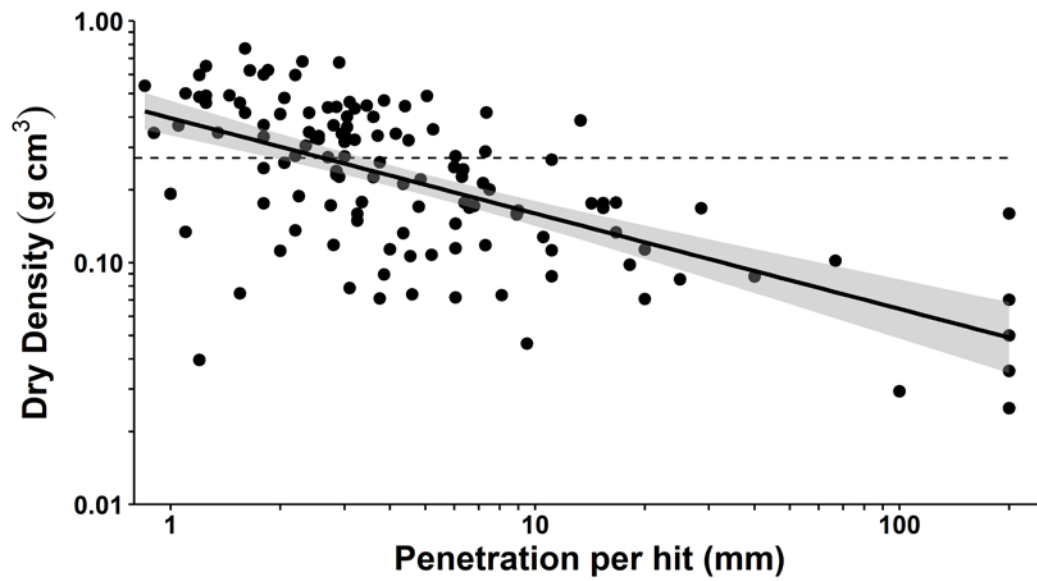


Fig. S6. Regression and 95% confidence interval of CWD dry density (g cm^3 , calculated using extracted disks) and penetrometer penetration (mm per hit). The dashed line represents average density across all samples (0.271 g m^3).

Table S1. Estimated residence times (means with 95% CI from individualized residence times) of downed and standing CWD under different assumptions regarding the density and diameter at the final census of pieces of CWD that fell below the measurement threshold at the final census (and thus were not remeasured). For the weighted residence time estimates, each decomposition constant was weighted by the mass or cross-sectional mass (rescaled from 0-1) of each piece of standing or downed CWD, respectively.

CWD pool	Assumed density at final census	Assumed diameter at final census	Unweighted residence time (years)	Weighted residence time (years)
Downed CWD	100%	199 mm	2.10 (1.97, 2.24)	15.29 (13.19, 17.86)
	100%	100 mm	1.03 (0.97, 1.09)	9.39 (8.33, 10.53)
	50%	199 mm	1.38 (1.30, 1.46)	11.61 (10.2, 13.22)
	100%	1 mm	0.23 (0.22, 0.25)	2.62 (2.42, 2.84)
	1%	199 mm	0.47 (0.44, 0.49)	4.93 (4.47, 5.44)
	1%	1 mm	0.16 (0.15, 0.17)	1.85 (1.69, 2.00)
Standing CWD	100%	199 mm	1.28 (1.19, 1.38)	29.24 (21.4, 42.28)
	100%	100 mm	0.60 (0.56, 0.64)	18.19 (13.39, 25.18)
	50%	199 mm	0.91 (0.85, 0.97)	23.95 (17.65, 33.7)
	100%	1 mm	0.14 (0.13, 0.15)	5.1 (3.98, 6.49)
	1%	199 mm	0.35 (0.33, 0.37)	11.85 (9.14, 15.8)
	1%	1 mm	0.1 (0.09, 0.11)	3.87 (3.13, 4.85)

Table S2: Estimates of downed CWD, standing CWD, standing FWD, suspended CWD, and suspended FWD pools based on data from the dynamics plots from 2009 to 2016, with 95% confidence intervals from bootstrapping over sampling units, together with information on the total number of pieces encountered and the proportion of samples without any pieces encountered. Sampling units are 10-m transect sections for downed WD, 10x10 m subplots for standing and suspended WD, and 5m radius plots for standing FWD.

Pool	Year	Total WD pieces	Samples without WD (%)	Volume (m ³ ha ⁻¹)	Mass, penetrometer (Mg ha ⁻¹)	Mass, average density (Mg ha ⁻¹)
Downed CWD	2009	230	88.7	43.8 (32.2, 57.9)	11.7 (8.5, 15.6)	11.9 (8.7, 15.7)
	2010	258	87.6	51.5 (39.3, 64.8)	12.7 (9.4, 16.3)	13.9 (10.7, 17.6)
	2012	242	87.7	40.8 (31.0, 52.4)	10.6 (8.2, 13.0)	11.1 (8.4, 14.2)
	2013	272	86.5	44.7 (33.9, 56.7)	11.6 (9.0, 14.7)	12.1 (9.2, 15.4)
	2014	260	87.4	47.1 (34.1, 63.3)	11.6 (8.7, 15.0)	12.8 (9.2, 17.2)
	2015	254	87.4	47.3 (33.7, 69.2)	11.7 (9.4, 14.7)	12.8 (9.1, 18.7)
	2016	255	87.5	41.9 (31.2, 55.1)	11.0 (8.3, 14.2)	11.4 (8.5, 14.9)
	All years	1766	87.5	45.3 (40.8, 50.7)	11.5 (10.3, 12.7)	12.3 (11.1, 13.7)
Standing CWD	2009	93	94.6	14.6 (6.9, 27.3)	5.9 (2.6, 11.9)	4.0 (1.9, 7.4)
	2010	120	93.2	16.7 (7.4, 30.4)	5.2 (2.8, 8.7)	4.5 (2.0, 8.2)
	2012	97	94.2	6.7 (4.7, 9.2)	2.2 (1.5, 3.2)	1.8 (1.3, 2.5)
	2013	123	92.9	9.6 (6.6, 13.4)	3.3 (2.2, 4.7)	2.6 (1.8, 3.6)
	2014	143	91.7	13.7 (8.9, 21.0)	4.7 (2.9, 7.5)	3.7 (2.4, 5.7)
	2015	143	91.9	11.7 (8.4, 15.5)	4.1 (2.9, 5.5)	3.2 (2.3, 4.2)
	2016	136	92.3	12.5 (8.4, 17.9)	4.7 (2.9, 6.8)	3.4 (2.3, 4.9)
	All years	855	93	12.2 (10.1, 15.2)	4.3 (3.5, 5.4)	3.3 (2.7, 4.1)
Suspended CWD	2015	22	90	0.23 (0.12, 0.37)	N/A	0.06 (0.03, 0.10)
Suspended FWD	2015	234	42.5	0.62 (0.48, 0.78)	N/A	0.17 (0.13, 0.21)
Standing FWD	All years	97	87	0.004 (0.003, 0.01)	N/A	0.001 (0.001, 0.002)

Table S3. The volume and three different mass estimates (penetrometer, average density, and extracted disk methods, $\pm 95\%$ CI) of downed CWD and FWD from long transects on BCI (20m sub-transects). Pools of woody debris are separated by their diameter at the point where they intersect the transect.

Year	Pool	Total WD pieces	Samples without WD (%)	Volume (m ³ ha ⁻¹)	Mass, penetrometer (Mg ha ⁻¹)	Mass, average density (Mg ha ⁻¹)	Mass, extracted disk (Mg ha ⁻¹)
2010	FWD (<20cm)	176	85.3	14.39 (10.69, 18.68)	N/A	3.90 (2.90, 5.06)	3.41 (2.24, 4.77)
	CWD (>20cm)	137	87.1	46.64 (30.24, 65.00)	11.78 (7.28, 17.41)	12.63 (8.20, 17.62)	11.64 (6.55, 18.83)
2014	FWD (<20cm)	161	87.1	19.64 (14.05, 26.80)	N/A	5.32 (3.81, 7.26)	N/A
	CWD (>20cm)	136	87.5	34.31 (25.81, 44.05)	8.25 (6.30, 10.47)	9.29 (6.99, 11.94)	N/A
2017	FWD (<10cm)	329	71.7	10.59 (8.77, 12.68)	N/A	2.87 (2.38, 3.44)	N/A
	CWD (>10cm)	561	44.3	60.45 (37.37, 97.62)	N/A	16.38 (10.13, 26.46)	N/A
	CWD (10-20cm)	314	71.2	5.38 (4.61, 6.16)	N/A	1.46 (1.25, 1.67)	N/A
	CWD (>20cm)	247	75.7	55.07 (33.46, 91.34)	N/A	14.92 (9.07, 24.75)	N/A

Table S4: Annual inputs of downed and standing CWD volume, penetrometer mass, and average density-based mass ($\pm 95\%$ CI) from the dynamics plots from 2009 to 2016. The majority of inputs occurred during the year identified below, but pieces of CWD were not surveyed until the first two months of the subsequent year. Input values were either calculated as intact inputs using equations for total woody biomass or corrected to account for mass and volume lost between the time that woody debris was input and the time it was first recorded.

Pool	Year	Total WD pieces	Samples without WD (%)	Volume ($\text{m}^3 \text{ha}^{-1}$)	Mass, penetrometer (Mg ha^{-1})	Mass, average density (Mg ha^{-1})
Downed	2009	75	96.3	11.9 (7.7, 17.3)	2.9 (1.8, 4.1)	3.2 (2.1, 4.7)
	2013	95	95.1	13.3 (9.2, 18.4)	4.0 (2.7, 5.3)	3.6 (2.5, 5)
	2014	63	97	15.8 (6.0, 33.4)	3.6 (1.5, 6.7)	4.3 (1.6, 9.1)
	2015	59	96.8	9.7 (5.9, 14.3)	2.9 (1.7, 4.4)	2.6 (1.6, 3.9)
	2016	67	96.6	15.1 (6.9, 28.3)	4.2 (2.0, 8.0)	4.1 (1.9, 7.7)
	All years	359	96.4	13.2 (9.8, 17.6)	3.5 (2.6, 4.5)	3.6 (2.7, 4.8)
Standing, Corrected	2010	46	97.2	6.3 (2.4, 11.4)	2.4 (0.9, 4.2)	1.7 (0.7, 3.1)
	2013	61	96.3	6.1 (3.2, 9.5)	2.2 (1.2, 3.6)	1.6 (0.9, 2.6)
	2014	53	96.7	4.4 (0.6, 11.6)	1.6 (0.2, 4.6)	1.2 (0.1, 3.1)
	2015	56	96.8	5.1 (2.6, 7.9)	1.9 (1, 2.9)	1.4 (0.7, 2.1)
	2016	35	97.9	5.6 (2.2, 10.8)	2.3 (0.9, 4.6)	1.5 (0.6, 2.9)
	All years	307	96.3	5.5 (3.7, 7.8)	2.1 (1.5, 2.9)	1.5 (1, 2.1)
Standing, Intact	2010	46	97.2	11.4 (4.8, 21.2)	4.1 (1.7, 7.6)	3.1 (1.3, 5.7)
	2013	61	96.3	15.2 (6.7, 26.9)	4.9 (2.5, 8.1)	4.1 (1.8, 7.3)
	2014	53	96.7	10.3 (1.6, 22.9)	3.5 (0.5, 8.2)	2.8 (0.4, 6.2)
	2015	56	96.8	8.5 (5.0, 12.7)	3.0 (1.8, 4.4)	2.3 (1.3, 3.4)
	2016	35	97.9	9.3 (4.1, 15.9)	3.5 (1.5, 6.3)	2.5 (1.1, 4.3)
	All years	307	96.3	11.0 (7.5, 14.8)	3.8 (2.6, 5.1)	3.0 (2.0, 4.0)

Table S5: The sample size, mass, and volume ($\pm 95\%$ CI) of downed WD inputs separated into branchfall and treefall. Estimates for 2015 and 2016 were based on inputs of CWD into the dynamics plots, with mass calculated using penetrometer measurements, whereas 2017 estimates were based on the volume of WD stocks characterized using long transects. These are the only datasets that separated branchfall and treefall inputs.

Stocks or Inputs	Year	Woody Debris Pool	Branchfall			Treefall			Branchfall WD (% of Total)		
			N	Volume m ³ ha ⁻¹ (95% CI)	Mass Mg ha ⁻¹ (95% CI)	N	Volume m ³ ha ⁻¹ (95% CI)	Mass Mg ha ⁻¹ (95% CI)	N	Volume	Mass
Inputs	2015	>20cm inputs	14	1.37 (0.36, 3.06)	0.50 (0.10, 1.36)	43	6.39 (3.45, 9.84)	1.76 (0.95, 2.73)	25	18 (5, 36)	22 (4, 46)
	2016	>20cm inputs	10	0.62 (0.23, 1.13)	0.20 (0.07, 0.34)	52	10.89 (4.18, 21.58)	2.99 (1.23, 5.73)	16	5 (2, 15)	6 (2, 17)
	2015-2016	>20cm inputs	24	1.00 (0.42, 1.81)	0.35 (0.13, 0.71)	95	8.64 (4.69, 14.19)	2.38 (1.36, 3.79)	20	10 (4, 22)	13 (4, 28)
Stocks	2017	2-10cm stocks	210	6.47 (5.03, 8.06)	N/A	26	1.68 (0.94, 2.51)	N/A	89	79 (70, 88)	N/A
		10-20cm	158	2.58 (2.04, 3.12)	N/A	145	2.63 (2.08, 3.2)	N/A	48	49 (45, 53)	N/A
		>20cm	33	2.17 (1.3, 3.1)	N/A	198	50.96 (29.09, 84.34)	N/A	14	4 (3, 6)	N/A
		>10cm stocks	191	4.75 (3.76, 6.00)	N/A	343	53.59 (31.28, 86.48)	N/A	36	8 (5, 13)	N/A
		>2cm stocks	401	11.22 (9.4, 13.16)	N/A	369	55.27 (33.95, 89.83)	N/A	52	17 (11, 26)	N/A

Table S6: The sample size, mass, and volume ($\pm 95\%$ CI) of downed CWD *treefall* inputs separated into branch wood and trunk wood. Estimates from 2015 and 2016 were based on inputs of CWD into the dynamics plots, with mass was calculated using penetrometer measurements, whereas 2017 estimates are based on the volume of WD stocks characterized using long transects.

Stocks or Inputs	Year	Woody Debris Pool	Branch wood			Trunk wood			Branch wood (% of total treefall)		
			N	Volume m ³ ha ⁻¹ (95% CI)	Mass Mg ha ⁻¹ (95% CI)	N	Volume m ³ ha ⁻¹ (95% CI)	Mass Mg ha ⁻¹ (95% CI)	N	Volume	Mass
Inputs	2015	>20cm	5	0.34 (0.06, 0.72)	0.09 (0.02, 0.18)	35	5.88 (3.16, 9.59)	1.62 (0.83, 2.59)	12	5 (1, 13)	5 (1, 11)
	2016	>20cm	17	1.32 (0.40, 2.64)	0.48 (0.14, 0.94)	35	9.58 (3.29, 20.03)	2.50 (0.79, 5.22)	33	12 (4, 35)	16 (4, 41)
	2015-2016	>20cm	22	0.83 (0.35, 1.47)	0.29 (0.11, 0.50)	70	7.73 (3.93, 13.62)	2.06 (1.04, 3.55)	24	10 (4, 20)	12 (5, 25)
Stocks	2017	2-10cm stocks	3	0.41 (0.0, 0.97)	N/A	22	1.26 (0.64, 1.91)	N/A	12	96 (95, 98)	N/A
		10-20cm	48	0.75 (0.46, 1.09)	N/A	97	1.88 (1.48, 2.33)	N/A	33	29 (24, 34)	N/A
		>20cm	32	2.84 (1.46, 4.54)	N/A	166	48.12 (26.58, 84.56)	N/A	16	6 (4, 8)	N/A
		>10cm stocks	80	3.59 (2.13, 5.28)	N/A	263	50.0 (27.87, 89.54)	N/A	23	7 (3, 12)	N/A
		>2cm stocks	83	4.0 (2.31, 6.06)	N/A	285	51.26 (29.18, 86.1)	N/A	23	7 (4, 13)	N/A

Table S7. The best fit distribution for the stocks and inputs of downed and standing CWD at the 10-m and 100m² scales, respectively, in each year that it was measured. The size parameter and standard error represent the overdispersion “size” parameter (k) for the negative binomial distribution when it fit the data similarly to or better than the Poisson distribution.

Year	Downed CWD				Standing CWD			
	Stocks Distribution	Size parameter (Std. Error)	Inputs Distribution	Size parameter (Std. Error)	Stocks Distribution	Size parameter (Std. Error)	Inputs Distribution	Size parameter (Std. Error)
2009	Negative Binomial	0.34 (0.07)	N/A	N/A	Negative Binomial	0.69 (0.48)	N/A	N/A
2010	Negative Binomial	0.35 (0.07)	Negative Binomial	0.09 (0.03)	Negative Binomial	0.59 (0.29)	Similar	0.59 (0.29)
2012	Negative Binomial	0.48 (0.12)	N/A	N/A	Similar	2.62 (4.86)	N/A	N/A
2013	Negative Binomial	0.46 (0.10)	Negative Binomial	0.15 (0.05)	Negative Binomial	0.80 (0.49)	Similar	0.80 (0.48)
2014	Negative Binomial	0.38 (0.08)	Negative Binomial	0.06 (0.02)	Similar	1.43 (1.10)	Poisson	-
2015	Negative Binomial	0.44 (0.10)	Negative Binomial	0.16 (0.07)	Negative Binomial	0.73 (0.36)	Negative Binomial	0.19 (0.11)
2016	Negative Binomial	0.36 (0.07)	Negative Binomial	0.07 (0.02)	Negative Binomial	0.82 (0.46)	Similar	0.22 (0.20)

Table S8. The coefficient of variation (CV, with 95% CI) and the overdispersion “size” parameter of the negative binomial distribution (\pm SE). Scale represents the sampling unit used for each estimate (10 m or 100 m²) and samples without WD denotes the percent of 10 m transects or 100 m² plots without a piece of CWD. The CV is the percent of the standard deviation over the mean of total volume or mass per transect, whereas the overdispersion parameter is based on the number of CWD pieces encountered per transect.

Pool or flux	Inputs or Stocks	Scale	Samples without WD (%)	Coefficient of variation		Overdispersion parameter
				Mass	Volume	
Downed CWD	Stocks	10m	87.6	550 (450, 660)	600 (470, 770)	0.4 (0.02)
		20m	77.3	390 (320, 470)	430 (320, 550)	-
		40m	65.5	320 (260, 390)	350 (270, 440)	-
		160m	22.2	160 (130, 200)	180 (160, 190)	-
	Inputs	10m	97.4	1220 (570, 1900)	1370 (550, 2310)	0.11 (0.02)
		20m	95.1	860 (420, 1370)	970 (420, 1600)	-
		40m	91.7	680 (300, 1080)	760 (310, 1300)	-
		160m	73.7	420 (190, 680)	320 (190, 820)	-
Standing CWD	Stocks	100m ²	92.9	1190 (640, 1870)	1210 (600, 1830)	1.1 (0.27)
		200m ²	86.8	840 (450, 1350)	860 (430, 1280)	-
		400m ²	75.6	600 (320, 930)	600 (320, 930)	-
		1600m ²	32.0	300 (170, 460)	310 (150, 470)	-
	Inputs	100m ²	97.0	1550 (870, 2450)	1580 (860, 2580)	0.77 (0.36)
		200m ²	94.2	1100 (630, 1800)	1110 (630, 1770)	-
		400m ²	88.9	770 (420, 1240)	790 (430, 1310)	-
		1600m ²	64.3	410 (240, 670)	410 (220, 690)	-

Supplemental References

- Chave J, Andalo C, Brown S, Cairns MA, Chambers JQ, Eamus D, Fölster H, Fromard F, Higuchi N, Kira T, Lescure JP, Nelson BW, Ogawa H, Puig H, Riéra B, Yamakura T. 2005. Tree allometry and improved estimation of carbon stocks and balance in tropical forests. *Oecologia* 145: 87-99.
- De Vries P. 1986. Sampling theory for forest inventory. a teach-yourself course. Berlin, Germany: Springer-Verlag.
- Kohyama TS, Kohyama TI, Sheil D. 2018. Definition and estimation of vital rates from repeated censuses: choices, comparisons and bias corrections focusing on trees. *Methods in Ecology and Evolution* 9: 809-821.
- Larjavaara M, Muller-Landau HC. 2011. Cross-section mass: an improved basis for woody debris necromass inventory. *Silva Fennica* 45: 291-298.
- Přívětivý T, Janík D, Unar P, Adam D, Král K, Vrška T. 2016. How do environmental conditions affect the deadwood decomposition of European beech (*Fagus sylvatica L.*)? *Forest Ecology and Management* 381: 177-187.